

Total Synthesis

Enantioselective Divergent Synthesis of (–)-*cis*- α - and (–)-*cis*- γ -Irene by Using Wilkinson's CatalystSerena Bugoni, Debora Boccato, Alessio Porta,* Giuseppe Zanoni, and Giovanni Vidari*^[a]Dedicated to Professor Paul A. Grieco on the occasion of his 70th anniversary

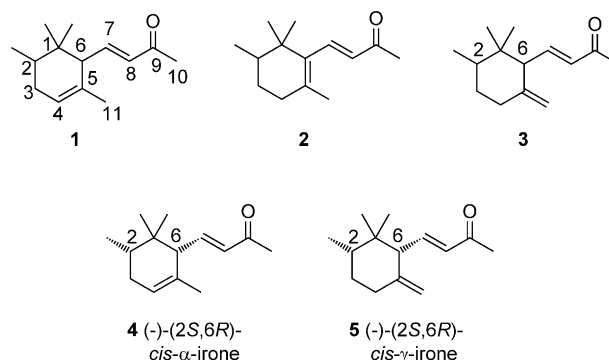
Abstract: A simple, efficient synthesis is reported for (–)-*cis*- α - and (–)-*cis*- γ -irone, two precious constituents of iris oils, in $\geq 99\%$ diastereomeric and enantioselective ratios. The two routes diverge from a common intermediate prepared from (–)-epoxygeraniol. Of general interest in this approach is the installation of the enone moiety of irones through a NHC–Au^I-catalyzed Meyer–Schuster-like rearrangement of a propargylic benzoate and the use of Wilkinson's catalyst for the stereoselective hydrogenation of a prostereogenic exocyclic double bond to secure the critical *cis* stereochem-

istry of the alkyl groups at C2 and C6 of the irones. The stereochemical aspects of this reaction are rationally supported by DFT calculation of the conformers of the substrates undergoing the hydrogenation and by a modeling study of the geometry of the rhodium η^2 complexes involved in the diastereodifferentiation of the double bond faces. Thus, computational investigation of the η^2 intermediates formed in the catalytic cycle of prostereogenic alkene hydrogenation by using Wilkinson's catalyst could be highly predictive of the stereochemistry of the products.

Introduction

Irones are C₁₄ nor-terpenoids, which impart a powerful and pleasant violet-like scent to the essential oil of *Iris* rhizomes.^[1] They have a long history in the chemistry of natural products and odorants. Indeed, from the 16th century, with the invention of the fragrance “Queen's water” at the French royal court of Catherine de' Medici, the scent of *Iris* extracts, obtained from orris roots through expensive and years-long processes, have continued to impart a delicate violet tone to many expensive fragrances, perfumes, and cosmetics, even nowadays.^[2] For example, the oil of the Italian *Iris pallida* donates the *boisé* note to *Armani Privé Nuances*, a high-priced unisex fragrance launched by Giorgio Armani in 2013.

Three double-bond regioisomers α , β , and γ (1–3; Figure 1) are present in different proportions in most iris oils, and iris oils of different origin show different enantiomeric composition of the three regioisomers.^[3] *cis*- α -irone and *cis*- γ -irone are the major components of the oils, while *trans*- α -irone has been found in minor amounts and *trans*- γ -irone is even rarer.^[3b,f] In addition, *Iris* plants of different geographical origin afford oils with different enantiomeric composition of the three regioisomers. For example, the dextrorotatory irones characterize the oil of Italian *Iris pallida* varieties, whereas the

Figure 1. Components of *Iris* oil.

levorotatory enantiomers that obtained from Moroccan *I. germanica*.^[3d] Notably, the human nose is able to distinguish the odor potency and characters of each of the ten irone isomers.^[3g] Thus, (–)-(2*S*,6*R*)-*cis*- α -irone **4** and (–)-(2*S*,6*R*)-*cis*- γ -irone **5** (Figure 1) have been determined to be stronger odorants than their enantiomers and their *trans*-stereoisomers, and (–)-*cis*- α -irone (**4**) shows the finest and strongest “orris-butter” character.^[4] Therefore, the synthesis of the single enantiomers **4** and **5** has long been a target for organic chemists. Fuganti and co-workers were able to prepare the single stereoisomers of the three regioisomeric irones, including **4** and **5**, by using the commercial product Irone Alpha. The process was, however, rather long and tedious, requiring multiple lipase-mediated resolutions of racemic mixtures and separation of diastereomeric products.^[4,5] Ex novo enantioselective synthesis of (–)-**4** and (–)-**5** was even more challenging, since the severe 1,3-al-

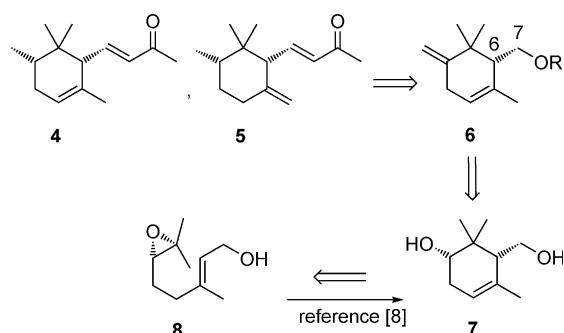
[a] S. Bugoni, D. Boccato, Dr. A. Porta, Prof. G. Zanoni, Prof. G. Vidari
Dipartimento di Chimica, Sezione Chimica Organica,
Università degli Studi di Pavia, Via Taramelli 12, 27100 Pavia (Italy)
E-mail: alessio.porta@unipv.it
vidari@unipv.it

Supporting information for this article is available on the WWW under
<http://dx.doi.org/10.1002/chem.201404642>.

lytic interaction^[6] between the substituents at C5 and C6 of the irone skeleton required the invention of ingenious strategies for installing the *cis* stereochemistry between H2 and H6. Moreover, enantioenriched optimal starting materials were seldom easily available. These difficulties account for the very few syntheses of **4** and **5** published to date.^[7]

Results and Discussion

We initially envisioned a novel and simple approach (Scheme 1) to install the critical *cis* stereochemistry of **4** and **5**



Scheme 1. Retrosynthesis of irones **4** and **5**.

in the regioselective and stereoselective hydrogenation of the exocyclic double bond of diene **6**. An added value of this strategy was the ready availability and excellent enantiomeric purity of the starting material. In fact, diol (–)-**7** can readily be obtained at $\geq 99\%$ *ee* by electrophilic cyclization of (–)-epoxygeraniol **8**, followed by crystallization.^[8]

Our assumption that hydrogen addition to the exocyclic double bond of a diene of general formula **6** would deliver the resulting methyl group at C2 in *cis* fashion to the substituent at C6 was predicted by exploration of the conformational space of model diene **9**. In fact, we envisioned that, in the absence of significant electronic effects displayed by the silyloxy substituent, the different steric hindrance of the two faces of the *exo* double bond would be the predominant factor controlling the reaction stereoselectivity. Indeed, calculations (see below) suggested that the face *syn* to H6 was more accessible than the *anti* face of the *exo* double bond, thus leading to the desired stereochemistry.

Modeling studies

The conformational space of compound **9** was explored by using the B3LYP functional. The symmetrical Me₃Si group was selected as the alcohol protecting group to facilitate the modeling study. All atoms were described with the 6-31+G(d,p) basis set,^[9] with the polarizable continuum model.^[10] Vibrational frequencies were computed at the same level of theory to verify that the optimized structures were minima. Calculations showed that diene **9** exists in two sets of low-energy conformations, a boat-like **S1** and a twist-chair-like **S2**, separated by a gap of about 6 kcal mol⁻¹ (1 kcal = 4.184 kJ) with each com-

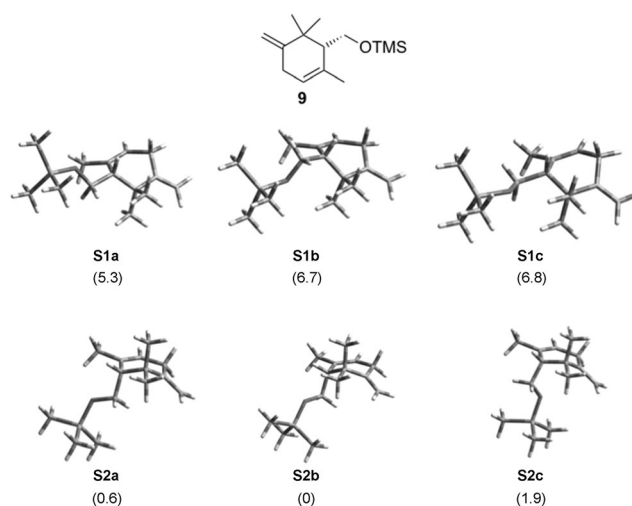


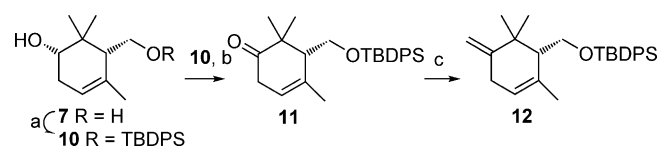
Figure 2. Structure of model diene **9** and 3D representations of its calculated boat (**S1 a–c**) and twist-chair conformations (**S2 a–c**). The relative energy (kcal mol⁻¹) of each conformer is shown within parentheses.

prising three rotamers **a–c** resulting from free rotation around the C6–C7 bond (Figure 2).

However, on the basis of the relative energies, it can be concluded that only conformers **S2 a–c** were significantly populated at room temperature.

Inspection of the most representative geometry of diene **9** clearly showed two sterically well-differentiated faces of the *exo* double bond, with the lower (*si,si'*) face severely obstructed by the pseudo-axial silyloxymethyl group, while the upper (*re,re'*) face was mainly hindered by the pseudoaxial methyl group at C1. However, due to the bent shape of the molecule, the *endo* approach to the double bond appeared to be more difficult than the *exo* approach, indicating that the *cis* product would be favored in addition reactions to the exocyclic double bond of **9**.

For synthetic purposes, a protecting group of the primary alcohol more robust than TMS was used. Conversion of diol **7** to substrate **12** was carried out straightforwardly in three standard steps (Scheme 2). Regioselective protection of **7** with *tert*-



Scheme 2. Conversion of diol **7** to *exo* olefin **12**: a) TBBDPSCI, Im, DMAP, DCM, room temperature, 2 h, 100% yield; b) TPAP, NMO, 4 Å molecular sieves, DCM, room temperature, 3 h, 78% yield; c) Ph₃PCH₃Br, NaN(SiMe₃)₂, THF, 70 °C, 20 h, 82% yield.

butyldiphenylsilyl chloride (TBBDPSCI) yielded silyl ether **10** quantitatively, which smoothly afforded ketone **11** in 78% yield upon exposure to *N*-methylmorpholine *N*-oxide (NMO) and catalytic tetra-*n*-propylammonium perruthenate (TPAP) in dichloromethane (DCM).^[11] Other oxidants such as pyridinium

chlorochromate (PCC) in DCM,^[12] Py-SO₃ in DMSO,^[13] or stabilized 2-iodoxybenzoic acid (SIBX) in DMSO,^[14] gave lower yields. Finally, Wittig reaction of **11** with the ylide generated from methyltriphenylphosphonium bromide and NaN(SiMe₃)₂ in THF, slowly produced the *exo* olefin **12**, isolated in 82% yield. An analogous route, by substituting TBDPSCI with *tert*-butyldimethylsilyl chloride (TBSCl) in the first step, afforded the corresponding TBS ether **13** in similar overall yields.

With dienes **12** and **13** in hand, we examined different protocols for adding hydrogen to the *exo* double bond in a regioselective and stereoselective fashion (Table 1). Diimide reduc-

Table 1. Results of hydrogen addition to dienes **12–14**.

Entry	Substrate	Reagents and catalysts	Solvent	T [°C]	Products (ratio) ^[a]	Yield [%] ^[b]
1	12	excess NH=NH from NH ₂ NH ₂ /H ₂ O ₂	MeOH/DCM	reflux	15/18 (4:1)	50
2	13	H ₂ , 5% Rh/Al ₂ O ₃	EtOAc	22	[c]	95
3	13	NiCl ₂ ·NaBH ₄	MeOH	0	16/19 (3:2)	90
4	12	NiCl ₂ ·NaBH ₄	MeOH	0	15/18 ^[d] (3:2)	90
5	12	H ₂ , 10% Pd/C	EtOAc	22	15/18 ^[e] (3.7:1)	95
6	12	H ₂ , [(Ph ₃ P) ₃ RhCl]	benzene	22	15/18 (9.5:1)	97
7	12	H ₂ , [(Ph ₃ P) ₃ RhCl]	DCM	22	15/18 (10.8:1)	96
8	14	H ₂ , [(Ph ₃ P) ₃ RhCl]	DCM	22	17/20 (7.3:1)	96

[a] Product ratio was determined by GC; [b] yield of isolated product; [c] mixture of tetrahydrostereoisomers; [d] accompanied by minor amounts of over-reduced products; [e] accompanied by 20% **21**.

tion of **12** (Table 1, entry 1) was completely regioselective, resulting in the production of the *cis* (**15**) and *trans* (**18**) products in the ratio of 4:1; however, the conversion was largely incomplete in spite of using excess reagent. Hydrogenation of **13** over 5% Rh on Al₂O₃ (Table 1, entry 2) was apparently highly *cis*-stereoselective (GC); however, at the end of the reaction, mainly the fully saturated product was formed, as an undetermined mixture of diastereomers. Exposure of **13** to nickel boride in MeOH (Table 1, entry 3) afforded a 60:40 mixture of *cis* and *trans* dihydroderivatives, **16** and **19**, while reduction of **12** with the same reagent (Table 1, entry 4) gave, in addition to **15** and **18**, a minor amount of unidentified over-reduced products. Hydrogenation of **12** in EtOAc over 10% Pd on carbon (Table 1, entry 5) afforded a 3.7:1 mixture of *cis* and *trans* dihydroderivatives, accompanied by 20% fully hydrogenated products **21**.

Finally, diene **12** was hydrogenated at room temperature in the presence of Wilkinson's catalyst [(Ph₃P)₃RhCl] (0.3 equiv) in carefully degassed benzene (Table 1, entry 6). On the basis of

DFT modeling studies (see below), we anticipated that complexation of substrate **12** with the rhodium center to give the active complex would be sterically demanding, resulting in a highly preferred coordination of the more accessible *exo* face (*re, re'*) of the less-hindered double bond of the diene, suggesting a highly regioselective reaction. Moreover, we expected the *cis* product **15** to be largely predominant, considering that, in the mechanism of the Wilkinson's hydrogenation,^[15] hydrogen ligands are transferred in *syn* fashion from the rhodium center to the coordinated double bond.

In the event, this hypothesis was confirmed by the isolation, in almost quantitative yield, of a mixture of **15** and **18**, in a ratio of 9.5:1 (GC; Table 1, entry 6), whereas no product from hydrogen addition to the trisubstituted olefin of **12** was detected. Wilkinson's hydrogenation showed a slightly higher diastereoselectivity in dichloromethane (Table 1, entry 7), affording **15** and **18** in a ratio of 10.8:1 (GC). In contrast, diastereoselectivity decreased for the hydrogenation of free alcohol **14** in DCM (Table 1, entry 8), confirming the importance of the bulky silyl group for sheltering the concave face of the disubstituted double bond.

Modeling study of epoxide **22** and synthesis of epoxides **23–25**

Although quite satisfactory, we considered the results of the hydrogenation of dienes **12–14** merely a confirmation of our hypothesis that steric factors encoded in the bent molecular shape and the pseudo-axial orientation of the silyloxymethyl substituent strongly determined the stereochemistry of products, mainly resulting from hydrogen addition to the disubstituted double bond of the substrate. By this reasoning, we expected that the *cis* diastereoselectivity of the hydrogenation would be improved significantly by increasing the steric hindrance around the *endo* (*si, si'*) face of the double bond. The 4,5-epoxides **24** and **25** were identified as the best candidates to test this hypothesis. In fact, the epoxy ring could be installed with high α -diastereoselectivity and regioselectivity on the trisubstituted double bond of diene **14**.^[16] Moreover, after the key hydrogenation step, the epoxy ring could be removed to restore the original double bond or serve as a useful synthetic linchpin (see below).

To gain some insight into the stereochemical features of epoxides **24** and **25**, we carried out a modeling study on the simpler homologue **22**. Calculations showed that **22** existed, in analogy with parent diene **9**, in two sets of low-energy conformations, a boat-like **S3** and a twist-chair-like **S4**, with an energy gap higher than 5 kcal mol⁻¹, and each comprising three rotamers **a–c** resulting from the free rotation around the C6–C7 bond (Figure 3). However, the relative energies clearly indicated that only conformers **S4 a–b** significantly represented the geometry of epoxide **22** at room temperature. We considered that the preference for this geometry should be largely independent of the silyl protecting group of the primary alcohol and, for synthetic purposes, we continued our work on TBDPS- or TBS-protected epoxides, **24** and **25**, respectively.

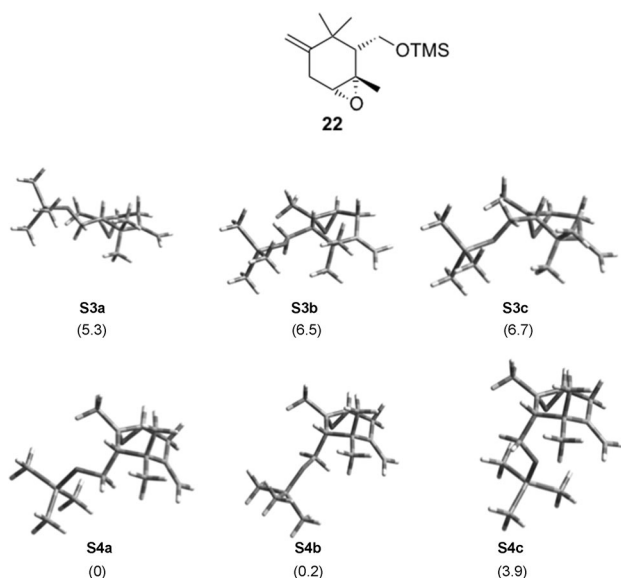
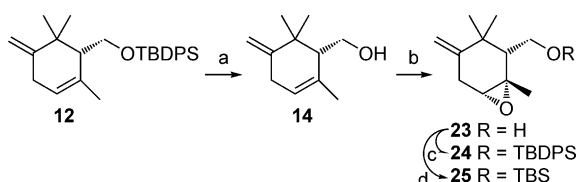


Figure 3. Structure of model epoxide **22** and 3D representations of its modeled boat (**S3a–c**) and twist-chair conformations (**S4a–c**). The relative energy (kcal mol⁻¹) of each conformer is shown between parentheses.

In the folded shape of compounds **24** and **25** the exocyclic methylene group was thus projected inside the molecular cavity even more deeply than in parent dienes **12** and **13**, respectively. This geometry and the additional steric hindrance created by the α -epoxy ring, were expected to hamper hydrogen addition to the *si,si'* face of the double bond of compounds **24** and **25** more efficiently than for dienes **12** and **13**. This would result in a higher proportion of 2,6-*cis* products. On the basis of this assumption, diene **12** was converted to **24** and **25** in a few simple steps (Scheme 3); however, to secure



Scheme 3. Conversion of diene **12** to epoxides **23–25**: a) TBAF, THF, room temperature, overnight, 100% yield. b) *m*-CPBA, DCM, 0 °C, 3 h, 74% yield. c) TBDPSCl, Im, DMAP, CH₂Cl₂, room temperature, 2 h, 100% yield. d) TBSCl, Im, CH₂Cl₂, room temperature, 2 h, 100% yield.

syn-epoxidation of the Δ^4 double bond to give the α -epoxide **23**, **12** had to be deprotected to the free alcohol **14**. As anticipated,^[16] epoxidation of **14** was completely regio- and diastereoselective, and configuration of the α -epoxide was confirmed by the NOESY spectrum of subsequent compound **27**.

Hydrogenation of epoxides **23–25**

Epoxides **23–25** were then submitted to the key hydrogenation reaction of the exocyclic double bond (Table 2). Both the reaction of epoxide **25** with 5% Rh/Al₂O₃ catalyst (Table 2,

Table 2. Results of hydrogenation of epoxides **23–25**.

The reaction scheme shows the hydrogenation of epoxides **23–25** to products **26–31**. The substituents are defined as: **23** R = H, **24** R = TBDPS, **25** R = TBS; **26** R = H, **27** R = TBDPS, **28** R = TBS; **29** R = H, **30** R = TBDPS, **31** R = TBS.

Entry	Substrate	Reagents and catalysts	Solvent	T [°C]	t [h]	Products (ratio) ^[a]	Yield [%] ^[b]
1	25	H ₂ , 5% Rh/Al ₂ O ₃	EtOAc	22	24	28:31 (3.5:1)	95
2	24	H ₂ , 10% Pd/C	EtOAc	22	24	27:30 (4.3:1)	N.D. ^[c]
3	24	H ₂ , [(Ph ₃ P) ₃ RhCl]	benzene, 22	22	7	27:30 ($\geq 99:1$)	94
4	24	H ₂ , [(Ph ₃ P) ₃ RhCl]	DCM	22	7	27:30 ($\geq 99:1$)	95
5	23	H ₂ , [(Ph ₃ P) ₃ RhCl]	DCM	22	7	26:29 (91:9)	96

[a] Product ratio was determined by GC; [b] yield of isolated product; [c] yield was not determined. Expected products were accompanied by considerable amounts of compounds in which the epoxy ring was cleaved.

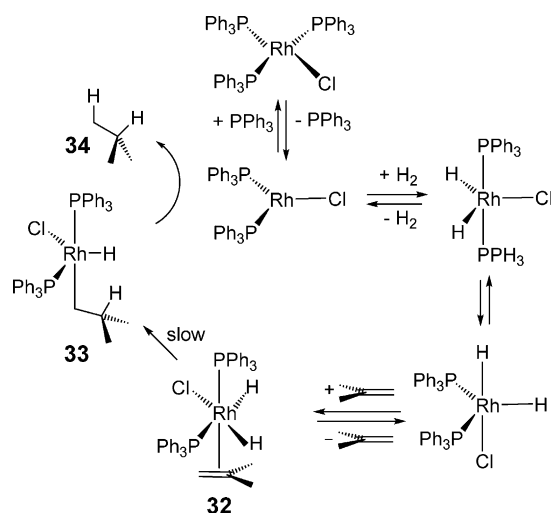
entry 1) and epoxide **24** with 10% Pd/C catalyst (Table 2, entry 2) proceeded with higher diastereoselectivity than with dienes **13** and **12** (Table 1, entries 2 and 5), respectively, as expected; however, the diastereomeric purities of *cis* diastereomers **28** and **27** were still unacceptably low.

In striking contrast, hydrogenation of **24** by using Wilkinson's catalyst (0.3 equiv) afforded the desired *cis* product **27** in an excellent $\geq 99:1$ diastereomeric ratio (GC), either in benzene (Table 2, entry 3) or in DCM (Table 2, entry 4). The relative stereochemistry of epoxide **27** was fully confirmed by the NOESY spectrum (see the Supporting Information) and the subsequent conversion to known alcohols **17** and **43** (see below). In contrast, as previously observed with diene **14**, Wilkinson's hydrogenation of the free alcohol **23** occurred with high but significantly lower diastereoselectivity (Table 2, entry 5) than with the bulky silyl ether **24**.

Modeling study of the Wilkinson's hydrogenation

To shed further light on the stereochemical aspects of the Wilkinson's hydrogenation of epoxide **24** and diene **12**, at first we carried out DFT modeling studies on the complexes formed by the rhodium catalyst with the model epoxide **22**. Calculations were carried out by DFT at the B3LYP^[9] and M06^[17] levels with a differentiated basis set in benzene as a solvent with polarizable continuum model.^[10] C, H, and O atoms were described by using the 6-31G(d) basis set, whereas Cl, Si, and P atoms were described with the 6-31+G(d,p) basis set and Rh atom with the LANL2DZ^[18] relativistic effective core potential basis set, by using the Gaussian 09 software suite.^[19]

Several different reaction mechanisms have been proposed for the Wilkinson's hydrogenation catalytic cycle, of which two "hydride route" mechanisms are believed to be the predominant pathways.^[15] However, the absence of a solvent effect on



Scheme 4. Hydride route mechanism proposed for the Wilkinson's hydrogenation of alkenes.^[15]

the reaction stereoselectivity (see above) and the steric hindrance of ligands tend to support the mechanism in which no solvent molecule is involved and the two phosphine ligands are *cis* oriented in the key η^2 intermediate **32** formed by coordination of a terminal olefin to rhodium (Scheme 4).^[15] Moreover, computational studies on the η^2 coordination complex of a model epoxide mimicking **22** (see the Supporting Information) indicated that the chloro ligand is spatially oriented far from the bulky geminal dimethyl group in the octahedral dihydride alkene complex. We assumed that such geometry is preserved also in the complexes with epoxides **22** and **24** (see below). According to the proposed mechanism (Scheme 4), the first four steps leading to **32** are considered to be fast equilibria, whereas the rate-determining alkene insertion (**32**→**33**) and the fast alkyl reductive elimination (**33**→**34**) are essentially irreversible steps.^[15] In the case of a prostereogenic olefin, such as **22**, the stereochemistry of hydrogenated products is determined by the olefin recognition step, namely by the face of the double bond that coordinates to rhodium in the key **32**-type η^2 intermediate. In fact, in both the alkene insertion (**32**→**33**) and the reductive elimination steps (**33**→**34**), the two hydrogens add in *syn* fashion to the face of the double bond that is initially coordinated to the rhodium center (Scheme 4).

Considering the two faces of the *exo* olefin and the two types of the most-populated conformations of epoxide **22** (Figure 3), four families of η^2 complexes could in principle be formed, each family comprising three different rotamers. However, a finite value of the energy could be calculated for only three types of η^2 complexes. In fact, rhodium coordination to the *si,si'* (*endo*) face of the twist-chair conformation of epoxide **22** was predicted not to form a stable complex. All of the stable complexes were modeled (see the Supporting Information); however, in Figure 4 we depict, as an example, only the geometries of the complexes between rhodium and the most stable rotamer of the two conformers.^[20] **35a** (Figure 4), resulting from complex formation on the *re,re'* face of the twist-chair

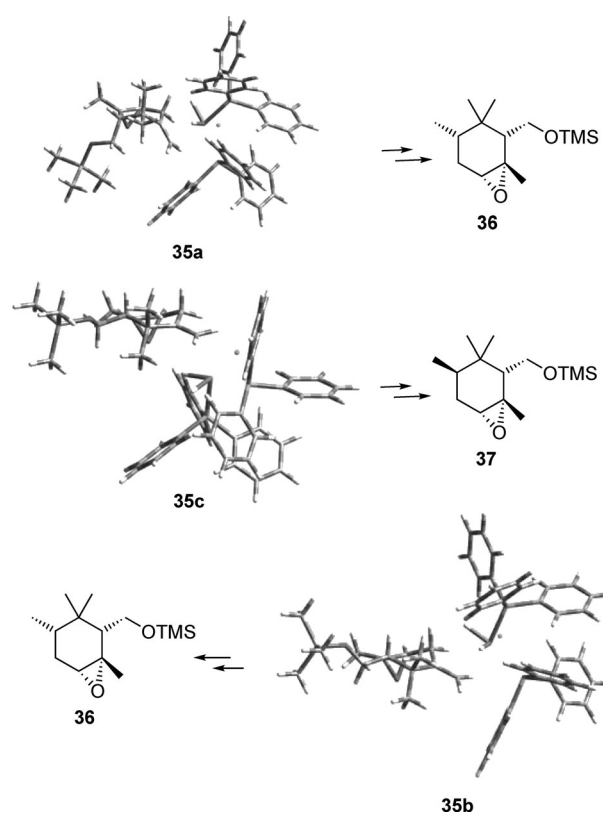


Figure 4. Computed *exo* and *endo* η^2 complexes of epoxide **22** in the twist-chair (**35a**) and boat conformations (**35b** and **c**).

conformation of **22** (Figure 3); **35b** (Figure 4), resulting from complex formation on the *re,re'* face of the boat conformation of **22** (Figure 3); **35c** (Figure 4), resulting from complex formation on the *si,si'* face of the boat conformation of **22** (Figure 3). Therefore, both **35a** and **35b** would give rise to the *cis*-hydrogenated product **36** at the end of the catalytic cycle, while the *trans*-hydrogenated product **37** would originate from the complex **35c**.^[20] Then, it was reasonable to assume that the steric and conformational effects present in the η^2 intermediates of type **32**, likely occurred also in the transition states of the olefin insertion step (**32**→**33**). Indeed, the calculated transition states for the Wilkinson's hydrogenation of epoxide **22** were of the early type and showed geometries very similar to the starting complexes (data not included). As a consequence, the difference in energy between the competitive transition states of olefin insertion was comparable with the relative energy of the η^2 intermediates. In this scenario, according to the Curtin-Hammett principle,^[21] the diastereoselectivity of the hydrogenation of the model epoxide **22** by using Wilkinson's catalyst could confidently be predicted on the basis of the relative stability of the η^2 complexes.

The energies of the different complexes **35a**–**c** in the gas phase and in benzene solution were thus determined at the B3LYP^[9] and M06^[17] levels (Table 3).^[20]

The calculations clearly indicated that **35a** would be, to a great extent, the most representative geometry of the η^2 intermediate in the Wilkinson's hydrogenation of epoxide **22**, whereas **35b** or **35c** would play an insignificant role or no role

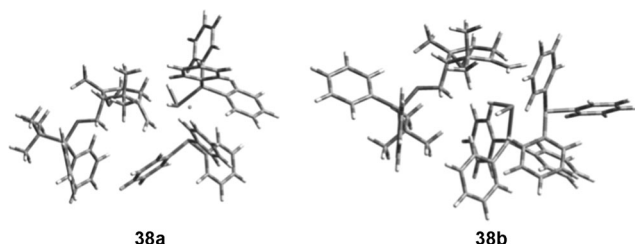
Table 3. Energies E (aU) and relative energies ΔE (kcal mol⁻¹) of complexes **35 a–c** calculated in gas phase and in benzene as a solvent.^[a]

Complex	$E^{[b]}$ (ΔE)	$E^{[c]}$ (ΔE)	$E^{[d]}$ (ΔE)	$E^{[e]}$ (ΔE)
35 a	-3632.66472 (0)	-3632.674516 (0)	-3630.953748 (0)	-3630.963414 (0)
35 b	-3632.653793 (+6.8)	-3632.664076 (+6.5)	-3630.936633 (+10)	-3630.946957 (+10)
35 c	-3632.654990 (+6.1)	-3632.665330 (+5.8)	-3630.924848 (+18)	-3630.935827 (+17)

[a] Cartesian Coordinates and complete Boltzmann distribution analyses of all structures are included in the Supporting Information; [b] calculated in gas phase at RB3LYP level; [c] calculated in benzene at RB3LYP level; [d] calculated in gas phase at M06 level; [e] calculated in benzene at M06 level.

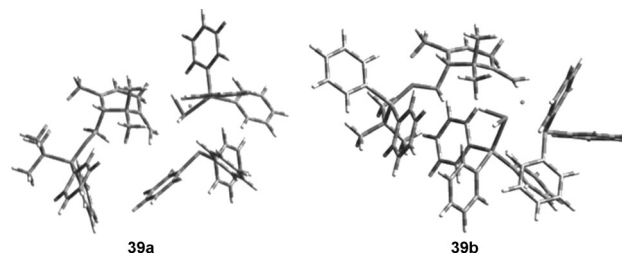
at all in the catalytic cycle. Therefore, the computational investigation on η^2 complexes of model epoxide **22** was highly indicative of the factors determining the almost complete *cis* diastereoselectivity for the homogeneous hydrogenation of epoxide **24**. To further support the experimental data, we then extended the modeling study to epoxide **24** itself, starting from the geometries found for the model **22**.

Only the η^2 intermediates **38 a** and **38 b** (Figure 5), resulting from complex formation on the *exo* and *endo* faces, respective-

**Figure 5.** Computed *exo* and *endo* η^2 complexes, **38 a** and **b**, respectively, of epoxide **24** in the twist-chair conformation with Wilkinson's catalyst.

ly, of the double bond in the largely most populated twist-chair conformer of compound **24**, were considered. Rather unexpectedly, contrary to the results found for the model epoxide **22**, the *endo* complex **38 b** also converged to a minimum (imaginary frequencies = 0) and its energy could be estimated. Indeed, the change of the TMS with the TBDPS group was accompanied by a significant change in the geometric parameters of the *endo* complex (see Supporting Information), so that severe repulsive interactions between the phosphine ligands and the substituents at silicon were partially alleviated. However the calculated energy difference between **38 a** and **38 b** remained very large (4.36 kcal mol⁻¹), in full agreement with the ratio $\geq 99:1$ of *cis* and *trans* hydrogenated products, **27** and **30**, formed from epoxide **24** (Table 2, entries 3 and 4).

For comparison, the two η^2 complexes **39 a** and **39 b** (Figure 6), resulting from coordination of the rhodium center to the *re, re'* and *si, si'* faces, respectively, of the exocyclic double bond of diene **12**, were also submitted to modeling studies. To simplify the calculations, only the most populated

**Figure 6.** Computed *exo* and *endo* η^2 complexes, **39 a** and **b**, respectively, of diene **12** in the twist-chair conformation with Wilkinson's catalyst.

twist-chair conformation of substrate **12** was considered. Cartesian coordinates and energies (aU) are reported in the Supporting Information.

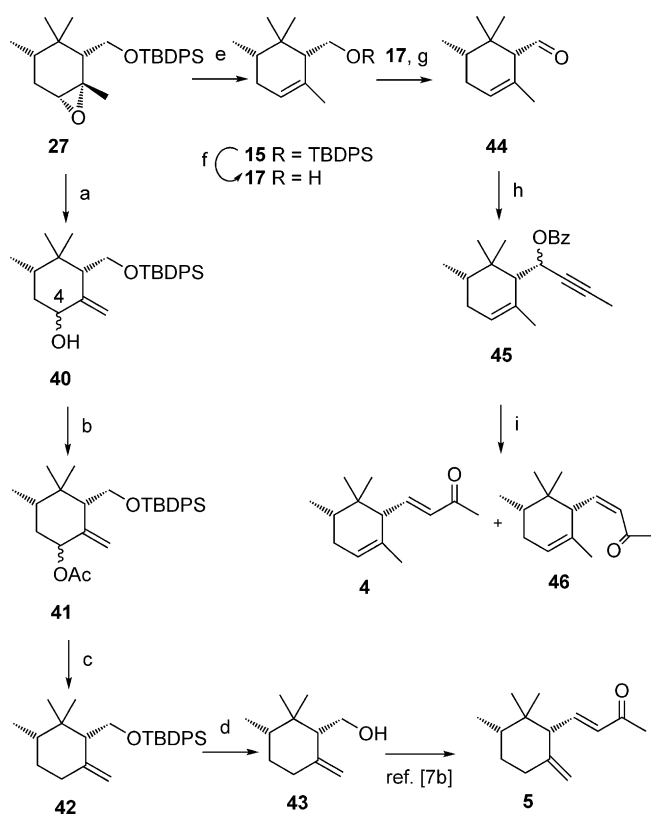
The calculated energy difference between the *exo* and *endo* complexes **39 a** and **39 b** was 1.3 kcal mol⁻¹, which corresponded to a product ratio of 9:1 (**15/18**), in good agreement with the experimental data obtained for the Wilkinson's hydrogenation of diene **12** (Table 1, entries 6 and 7).

Final steps of the syntheses of (–)- α -irone **4** and (–)- γ -irone **5**

With epoxide **27** securely in hand, the synthesis of irones **4** and **5** was completed through two straight divergent routes (Scheme 5). Isomerization of epoxide **27** to the corresponding allylic alcohol **40** was realized in excellent yield upon exposure to excess Al(O*i*Pr)₃ in refluxing xylene.^[16b] After acetylation of **40** to acetate **41**, the acetoxy group was removed by Pd-mediated hydride reduction to afford protected alcohol **42** in high yield.^[22] Deprotection of **42** under standard conditions yielded free alcohol **43**, identical with the literature,^[7b,d] in $\geq 99\%$ diastereomeric and enantiomeric purity by chiral HPLC analysis. Conversion of compound **43** to (–)- γ -irone **5** was then accomplished, with conservation of the stereoisomeric purity, by following a well-established procedure.^[7d,e]

To prepare an advanced intermediate for the synthesis of (–)- α -irone **4**, we first attempted direct isomerization of the *exo* olefin **42** to the thermodynamically more stable trisubstituted *endo* olefin **15**. However, upon treating **42** with I₂ in DCM or with H₃PO₄ in toluene at reflux, the desired compound was produced in unacceptable yields. In contrast, de-epoxidation of **27** by use of Zn powder and NaI,^[23] followed by cleavage of the silyl protecting group by using a standard protocol, delivered free alcohol **17**, identical with the literature,^[7b] in 76% overall yield, and $\geq 99\%$ e.r. and d.r. (GC).

It is well known that construction of an enone side chain, such as that present in α -irone, from a **17**-like alcohol precursor is not a trivial process. In fact, Wittig-like olefinations of corresponding **44**-type aldehydes, under non-racemizing conditions, proceeded with unacceptably low yields.^[8] Moreover, aldol homologation of aldehyde **44** with Me₂CO and EtONa occurred with considerable erosion of the *cis* stereochemistry.^[7b] To circumvent this problem, a few years ago we resorted to an alternative methodology based upon a Julia–Lythgoe olefination, although the synthetic sequence was significantly length-



Scheme 5. Synthesis of $(-)-(2S,6R)$ -*cis*- α -irone **4** and $(-)-(2S,6R)$ -*cis*- γ -irone **5** from epoxide **27**: a) $\text{Al}(\text{O}i\text{Pr})_3$, xylene at reflux, 12 h, 95%; b) Ac_2O , pyridine, DMAP, DCM, room temperature, 2 h, 98%; c) $[\text{Pd}(\text{PPh}_3)_4]$, Et_3N , HCO_2H , THF at reflux, 24 h, 83% yield; d) TBAF, THF, room temperature, overnight, 100% yield; e) Zn , NaOAc , NaI , AcOH , DCM, 40°C , 24 h, 76% yield; f) TBAF, THF, room temperature, overnight, 100% yield; g) SIBX , DMSO, room temperature, 2 h; h) 1-propynyl-magnesium bromide, THF, -78°C \rightarrow 0°C , 2 h, followed by BzCl , DMAP, 0°C \rightarrow 25°C , 2 h, 63% overall yield from **17**; i) $[(\text{IprAu})_2(\mu\text{-OH})]\text{BF}_4$, butan-2-one - H_2O , 100:1, 60°C , 12 h, 68% total yield of **4** + **46**, 70:15.

ened.^[8] More recently, we introduced an innovative methodology involving an NHC-Au^I ($\text{NHC} = N$ -heterocyclic carbene) catalyzed Meyer-Schuster-like rearrangement of propargylic esters,^[24] which was readily employed for the synthesis of the enone moiety of α -ionone.^[25] To extend this procedure also to the synthesis of α -irone, we oxidized alcohol **17** with SIBX ^[14] to the highly epimerizable aldehyde **44**, which, without purification, was immediately submitted to the addition of propynylmagnesium bromide in THF. Quenching the resulting alkoxy derivative with benzoyl chloride (BzCl), in the presence of a catalytic amount of 4-dimethylaminopyridine (DMAP), produced propargyl benzoate **45** in 63% yield (see the Supporting Information for the detailed procedure). The ester **45** was then exposed to the Nolan dinuclear NHC-Au^I catalyst $[(\text{IprAu})_2(\mu\text{-OH})]\text{BF}_4$ ^[26] in a 100:1 butan-2-one/ H_2O solvent mixture, at 60°C for 12 h. A 4.7:1 mixture of (E) - $(-)$ - α -irone **4** and (Z) - $(-)$ - α -irone **46**^[7a] was delivered in 68% combined yield. The two diastereomers were cleanly separated by chromatography on silica gel, and the (Z) -isomer **46** was then treated with I_2 in DCM to induce $Z \rightarrow E$ isomerization of the enone unit.^[27] The reaction was completed in 2 h; however, it produced, in quantitative

yield, a chromatographically inseparable mixture of (E) - $(-)$ - α -irone **4** and (E) - $(-)$ - β -irone **2**, in the ratio of 7:1 by NMR analysis. GC analysis of chemically pure (E) - $(-)$ - α -irone **4** indicated no loss of stereochemistry from starting alcohol **17**.

Conclusion

In conclusion, the extremely precious components of iris oils, $(-)-(2S,6R)$ -*cis*- α -irone (**4**) and $(-)-(2S,6R)$ -*cis*- γ -irone (**5**) have been obtained in enantiomeric and diastereomeric ratios of $\geq 99:1$ by following two simple synthetic pathways diverging from common epoxide **27**. This intermediate was prepared straightforwardly from $(-)$ -epoxygeraniol **8** through the cyclic diol $(-)$ -**7**. Since the enantiomer $(+)$ -**7** is obtainable from $(+)$ -epoxygeraniol,^[8] this synthetic pathway formally constitutes also the synthesis of the antipodes $(+)$ - $(2R,6S)$ -*cis*- α -irone and $(-)$ - $(2R,6S)$ -*cis*- γ -irone. Of general interest in our approach are the installation of the enone moiety of irones through an NHC-Au^I -catalyzed Meyer-Schuster-like rearrangement^[24] of a propargylic benzoate and the use of Wilkinson's catalyst for the stereoselective hydrogenation of a prostereogenic exocyclic double bond to secure the critical *cis* stereochemistry of the alkyl groups at C2 and C6 of irones. The stereochemical aspects of this reaction were rationally supported by DFT calculation of the conformers of the substrates undergoing the hydrogenation and by modeling study of the geometry of the rhodium η^2 complexes involved in the diastereodifferentiation of the double bond faces. The almost complete diastereoselectivity predicted by the calculations was confirmed well by the experimental data. They indicated that computational investigation of the η^2 intermediates formed in the catalytic cycle of alkene hydrogenation by using Wilkinson's catalyst could be highly predictive of the stereochemistry of products. In addition, our results support the hydride route mechanism with isomerization, proposed for homogeneous hydrogenation of alkenes by using Wilkinson's catalyst.^[15]

The novel synthetic pathway to enantioenriched *cis*- α -irone and *cis*- γ -irone disclosed herein competes favorably with existing synthetic routes in terms of simplicity and stereoselectivity.

Experimental Section

Wilkinson's hydrogenation of epoxide **24** to give *tert*-butyldiphenyl(((1*S*,2*R*,4*S*,6*R*)-1,3,3,4-tetramethyl-7-oxabicyclo[4.1.0]heptan-2-yl)methoxy)silane (**27**).

$[(\text{PPh}_3)_3\text{RhCl}]$ (206 mg, 0.2 mmol, 0.3 equiv) was added to a solution of epoxide **24** (313 mg, 0.7 mmol, 1.0 equiv) in degassed dry dichloromethane (7.4 mL). The mixture was exposed to H_2 (101 325 Pa) under magnetic stirring at room temperature for 7 h. After removal of volatiles under reduced pressure, the residue was separated by column chromatography (150 mm \times 30 mm) on silica gel (15 g; eluent = 2% Et_2O /hexane), affording epoxide **27** (296 mg, yield = 95%) as a colorless viscous oil. $R_f = 0.31$ (2% Et_2O /hexane); $[\alpha]_D^{22} = -12.3 \text{ cm}^3 \text{ g}^{-1} \text{ dm}^{-1}$ ($c = 1.3$ in CH_2Cl_2); $^1\text{H NMR}$ (300 MHz, CD_2Cl_2): $\delta = 7.75\text{--}7.55$ (m, 4H), $7.50\text{--}7.35$ (m, 6H), $4.12\text{--}3.78$ (m, 2H), 2.92 (d, $J = 2.9$ Hz, 1H), $1.93\text{--}1.84$ (m, 1H), $1.73\text{--}1.68$ (m, 1H), $1.59\text{--}1.53$ (m, 1H), 1.45 (s, 3H), $1.35\text{--}1.25$ (m, 1H), 1.09 (s, 9H), 0.82

(s, 3H), 0.78 (d, $J=5.2$ Hz, 3H), 0.65 ppm (s, 3H); ^{13}C NMR (75 MHz, CD_2Cl_2): $\delta=136.5$ (d), 136.4 (d), 134.5 (s), 130.4 (d), 130.3 (d), 128.4 (d), 64.2 (t), 62.2 (d), 60.5 (s), 52.1 (d), 38.8 (d), 35.2 (s), 30.7 (t), 29.2 (q), 27.4 (q), 25.1 (q), 19.7 (s), 16.7 (q), 16.2 ppm (q); IR (oil film on NaCl disks): $\tilde{\nu}=2962$, 1472, 1428, 1390, 1112, 856, 824, 740, 701 cm^{-1} ; HRMS (EI): m/z calcd for $\text{C}_{27}\text{H}_{38}\text{O}_2\text{Si}$: 422.2641; found 422.2645.

The diastereomeric ratio (d.r.) $\geq 99:1$ of compound **27** was determined by GC analysis on a capillary HP5 column (30 m, 0.25 mm i.d., 0.25 μm f.t.); carrier gas=He, flow=1 mL min^{-1} ; injector temperature=250 °C; detector: MS; temperature program: 80 °C (1 min), then 10 °C min^{-1} to 280 °C (5 min); t_{R} of *cis* compound **27**=21.44 min; t_{R} of *trans* compound **30**=21.04 min.

Meyer–Schuster rearrangement^[24] of propargylic benzoate **45**.

[(*lprAu*)₂OH]BF₄ (2.7 mg, 0.002 mmol, 0.02 equiv) was added to a solution of ester **45** (33 mg, 0.1 mmol, 1.0 equiv) in a 100:1 butan-2-one/H₂O solvent mixture (1.1 mL/0.011 mL). The mixture was stirred and heated at 60 °C for 12 h. The solvent was then removed under reduced pressure ($P > 10.66$ kPa). The residue, composed by a mixture of *E* and *Z* isomers, was separated by column chromatography (150 mm × 15 mm) on silica gel (5 g; eluent=1% Et₂O/pentane), affording (*Z*,2*S*,6*R*)-(–)-*cis*- α -irone **46** (2.6 mg, 12%) as a colorless oil, followed by the desired (*E*,2*S*,6*R*)-(–)-*cis*- α -irone **4** (12.3 mg, 56%) as a colorless oil.

(*E*,2*S*,6*R*)-(–)-*cis*- α -irone (**4**): The enantiomeric (e.r.) and diastereomeric ratio (d.r.) $\geq 99:1$ of compound **4** were determined by GC analysis on a capillary Mega DEX column (20 m, 0.25 mm i.d., 0.18 μm f.t.); dactnPentilSilBETACDX as stationary phase; carrier gas=He, split 1:30, flow=1 mL min^{-1} ; injector temperature=250 °C; detector: FID; temperature program: 80 °C (1 min), then 10 °C min^{-1} to 280 °C (5 min); $t_{\text{R}}=10.36$ min. $R_{\text{f}}=0.28$ (pentane-Et₂O, 99:1). $[\alpha]_{\text{D}}^{22}=-109.9$ $\text{cm}^3\text{g}^{-1}\text{dm}^{-1}$ ($c=0.42$ in CH_2Cl_2);^[7a] $[\alpha]_{\text{D}}^{21}=-119.2$ $\text{cm}^3\text{g}^{-1}\text{dm}^{-1}$ ($c=0.25$ in CH_2Cl_2);^[7b] $[\alpha]_{\text{D}}^{20}=-103.7$ ($c=0.65$ in CHCl_3 ; 86% ee);^[4] $[\alpha]_{\text{D}}^{20}=-130$ $\text{cm}^3\text{g}^{-1}\text{dm}^{-1}$ ($c=1.55$ in CH_2Cl_2 ; chemical purity=85%, 98% ee); ^1H NMR (300 MHz, CD_2Cl_2): $\delta=6.65$ (dd, $J=15.9$ and 10.8 Hz, 1H), 6.12 (d, $J=15.8$ Hz, 1H), 5.56 (m, 1H), 2.60 (br d, $J=10.0$ Hz, 1H), 2.25 (s, 3H), 2.05–1.95 (m, 1H), 1.87–1.70 (m, 1H), 1.53 (d, $J=1.6$ Hz, 3H), 1.55–1.45 (m, 1H), 0.88 (d, $J=6.5$ Hz, 3H), 0.87 (s, 3H), 0.71 ppm (s, 3H); ^{13}C NMR (75 MHz, CD_2Cl_2): $\delta=198.8$ (s), 150.1 (d), 135.5 (d), 133.2 (s), 123.9 (d), 57.0 (d), 39.0 (d), 36.7 (s), 32.8 (t), 27.9 (q), 27.7 (q), 23.7 (q), 16.2 (q), 15.8 ppm (q); IR (oil film on NaCl disks): $\tilde{\nu}=2965$, 1675, 1618, 1364, 1254, 966 cm^{-1} ; HRMS (EI): m/z calcd for $\text{C}_{14}\text{H}_{22}\text{O}$ 206.1671; found 206.1674. The ^1H NMR and ^{13}C NMR spectroscopic data of compound **4** are in accordance with those reported in the literature.^[7a,b]

(*Z*,2*S*,6*R*)-(–)-*cis*- α -irone (**46**): $R_{\text{f}}=0.32$ (1% Et₂O/pentane); $[\alpha]_{\text{D}}^{22}=-39$ $\text{cm}^3\text{g}^{-1}\text{dm}^{-1}$ ($c=1.3$ in CH_2Cl_2);^[7a] $[\alpha]_{\text{D}}^{21}=-37.7$ $\text{cm}^3\text{g}^{-1}\text{dm}^{-1}$ ($c=0.83$ in CH_2Cl_2); ^1H NMR (300 MHz, CD_2Cl_2): $\delta=6.37$ (d, $J=11.8$ Hz, 1H), 5.96 (t, $J=11.8$ Hz, 1H), 5.51 (m, 1H), 3.98 (br d, $J=11.7$ Hz, 1H), 2.23 (s, 3H), 1.94–1.86 (m, 1H), 1.75–1.67 (m, 1H), 1.55 (d, $J=1.5$ Hz, 3H), 1.35–1.25 (m, 1H), 0.89 (d, $J=6.8$ Hz, 3H), 0.87 (s, 3H), 0.71 ppm (s, 3H); ^{13}C NMR (75 MHz, CD_2Cl_2): $\delta=199.9$ (s), 148.5 (d), 133.7 (s), 130.4 (d), 122.8 (d), 50.2 (d), 38.8 (d), 36.7 (s), 32.7 (t), 32.5 (q), 26.9 (q), 23.0 (q), 15.0 (q), 14.6 ppm (q); HRMS (EI): m/z calcd for $\text{C}_{14}\text{H}_{22}\text{O}$ 206.1671; found 206.1675. The ^1H NMR spectrum of compound **46** is in complete accordance with the literature.^[7a]

Acknowledgements

We thank the Italian MIUR (funds PRIN) for financial support, and Professor Mariella Mella for the NMR spectra measurement.

Keywords: fragrances • hydrogenation • terpenoids • total synthesis • Wilkinson's catalyst

- [1] a) A. Tschirsch in *Handbuch der Pharmakognosie*, C. H. Tachnitz Verlag, Leipzig, **1917**, p. 1143; b) G. Ohloff, *Scent and Fragrances*; Springer-Verlag, Berlin, Heidelberg, **1994**, p. 164; c) L. Jaenicke, F. J. Marner, *Pure Appl. Chem.* **1990**, *62*, 1365–1368.
- [2] a) D. H. Pybus in *The Chemistry of Fragrances* (Eds.: D. H. Pybus, C. S. Sell), Royal Society of Chemistry, Cambridge, **1999**, p. 14; b) G. Ohloff, W. Pickenhagen, P. Kraft, *Scent and Chemistry: The Molecular World of Odors*, Wiley-VCH, Weinheim, **2012**, p. 214.
- [3] a) W. Krick, F. J. Marner, L. Jaenicke, *Helv. Chim. Acta* **1984**, *67*, 318–323; b) V. Rautenstrauch, B. Willhalm, W. Thommen, G. Ohloff, *Helv. Chim. Acta* **1984**, *67*, 325–331; c) F. J. Marner, L. Jaenicke, *Helv. Chim. Acta* **1989**, *72*, 287–294; d) F. J. Marner, T. Runge, W. A. König, *Helv. Chim. Acta* **1990**, *73*, 2165–2170; e) A. Galfré, P. Martin, M. Petrizlka, *J. Essent. Oil Res.* **1993**, *5*, 265–277; f) E. Brenna, C. Fuganti, S. Ronzani, S. Serra, *Helv. Chim. Acta* **2001**, *84*, 3650–3666; g) E. Brenna, C. Fuganti, S. Serra, *Tetrahedron: Asymmetry* **2003**, *14*, 1–42.
- [4] E. Brenna, C. Fuganti, S. Serra, *C. R. Chim.* **2003**, *6*, 529–546.
- [5] E. Brenna, C. Fuganti, S. Serra, *Chem. Soc. Rev.* **2008**, *37*, 2443–2451, and references therein.
- [6] R. W. Hoffmann, *Chem. Rev.* **1989**, *89*, 1841–1860.
- [7] (–)-*cis*- α -irone: a) Y. Ohtsuka, F. Itoh, T. Oishi, *Chem. Pharm. Bull.* **1991**, *39*, 2540–2544; b) C. Chapuis, R. Brauchli, *Helv. Chim. Acta* **1993**, *76*, 2070–2088; c) T. Inoue, H. Kiyota, T. Oritani, *Tetrahedron: Asymmetry* **2000**, *11*, 3807–3818; (–)-*cis*- γ -irone: references [7b] and [7c]; d) S. Beszant, E. Giannini, G. Zanoni, G. Vidari, *Eur. J. Org. Chem.* **2003**, 3958–3968; Formal synthesis: e) G. Laval, G. Audran, J.-M. Galano, H. Monti, *J. Org. Chem.* **2000**, *65*, 3551–3554.
- [8] M. Bovolenta, F. Castronovo, A. Vadalà, G. Zanoni, G. Vidari, *J. Org. Chem.* **2004**, *69*, 8959–8962.
- [9] a) A. D. Becke, *J. Chem. Phys.* **1993**, *98*, 5648–5652; b) C. Lee, W. Yang, R. G. Parr, *Phys. Rev. B* **1988**, *37*, 785–789.
- [10] J. Tomasi, B. Mennucci, R. Cammi, *Chem. Rev.* **2005**, *105*, 2999–3093.
- [11] W. P. Griffith, S. V. Ley, G. P. Whitcombe, A. D. White, *J. Chem. Soc. Chem. Commun.* **1987**, 1625–1627.
- [12] E. J. Corey, J. W. Suggs, *Tetrahedron Lett.* **1975**, *16*, 2647–2650.
- [13] J. R. Parikh, W. von E. Doering, *J. Am. Chem. Soc.* **1967**, *89*, 5505–5507.
- [14] A. Ozanne, L. Pouységu, D. Depernet, B. Francois, S. Quideau, *Org. Lett.* **2003**, *5*, 2903–2906.
- [15] D. J. Nelson, R. Li, C. Brammer, *J. Org. Chem.* **2005**, *70*, 761–767.
- [16] a) C. Fehr, *Angew. Chem. Int. Ed.* **1998**, *37*, 2407–2409; *Angew. Chem.* **1998**, *110*, 2509–2512. b) M. Luparia, P. Boschetti, F. Piccinini, A. Porta, G. Zanoni, G. Vidari, *Chem. Biodiversity* **2008**, *5*, 1045–1057.
- [17] Y. Zhao, D. G. Truhlar, *Theor. Chem. Acc.* **2008**, *120*, 215–241.
- [18] a) P. J. Hay, W. R. Wadt, *J. Chem. Phys.* **1985**, *82*, 270–283; b) P. J. Hay, W. R. Wadt, *J. Chem. Phys.* **1985**, *82*, 299–310; c) W. R. Wadt, P. J. Hay, *J. Chem. Phys.* **1985**, *82*, 284–298.
- [19] Gaussian 09, Revision B.01, M. J. Frisch, G. W. Trucks, H. B. Schlegel, G. E. Scuseria, M. A. Robb, J. R. Cheeseman, G. Scalmani, V. Barone, B. Mennucci, G. A. Petersson, H. Nakatsuji, M. Caricato, X. Li, H. P. Hratchian, A. F. Izmaylov, J. Bloino, G. Zheng, J. L. Sonnenberg, M. Hada, M. Ehara, K. Toyota, R. Fukuda, J. Hasegawa, M. Ishida, T. Nakajima, Y. Honda, O. Kitao, H. Nakai, T. Vreven, J. A. Montgomery, Jr., J. E. Peralta, F. Ogliaro, M. Bearpark, J. J. Heyd, E. Brothers, K. N. Kudin, V. N. Staroverov, T. Keith, R. Kobayashi, J. Normand, K. Raghavachari, A. Rendell, J. C. Burant, S. S. Iyengar, J. Tomasi, M. Cossi, N. Rega, J. M. Millam, M. Klene, J. E. Knox, J. B. Cross, V. Bakken, C. Adamo, J. Jaramillo, R. Gomperts, R. E. Stratmann, O. Yazyev, A. J. Austin, R. Cammi, C. Pomelli, J. W. Ochterski, R. L. Martin, K. Morokuma, V. G. Zakrzewski, G. A. Voth, P. Salvador, J. J. Dan-

- nenberg, S. Dapprich, A. D. Daniels, O. Farkas, J. B. Foresman, J. V. Ortiz, J. Cioslowski, D. J. Fox, Gaussian, Inc., Wallingford CT, **2010**.
- [20] From a qualitative point of view, the diastereoselectivity of the Wilkinson's hydrogenation predicted by our modeling studies did not change significantly upon taking into consideration also the complexes of rhodium with minor rotamers of epoxide **22**.
- [21] E. L. Eliel, S. H. Wilen, L. N. Mander, *Stereochemistry of Organic Compounds*, Wiley, Hoboken, **1994**, p. 647.
- [22] S. Serra, C. Fuganti, E. Brenna, *Helv. Chim. Acta* **2006**, *89*, 1110–1122.
- [23] D. E. Cane, G. Yang, R. M. Coates, H. J. Pyun, T. M. Hohn, *J. Org. Chem.* **1992**, *57*, 3454–3462.
- [24] a) N. Marion, P. Carlqvist, R. Gealageas, P. de Frémont, F. Maseras, S. P. Nolan, *Chem. Eur. J.* **2007**, *13*, 6437–6451; b) R. S. Ramón, N. Marion, S. P. Nolan, *Tetrahedron* **2009**, *65*, 1767–1773; c) D. A. Engel, G. B. Dudley, *Org. Biomol. Chem.* **2009**, *7*, 4149–4158.
- [25] V. Merlini, S. Gaillard, A. Porta, G. Zanoni, G. Vidari, S. P. Nolan, *Tetrahedron Lett.* **2011**, *52*, 1124–1127.
- [26] S. Gaillard, J. Bosson, R. S. Ramon, P. Nun, A. M. Z. Slawin, S. P. Nolan, *Chem. Eur. J.* **2010**, *16*, 13729–13740.
- [27] S. W. Hwang, M. Adiyaman, S. P. Khanapure, J. Rokach, *Tetrahedron Lett.* **1996**, *37*, 779–782.

Received: July 29, 2014

Published online on ■ ■ ■■, 0000

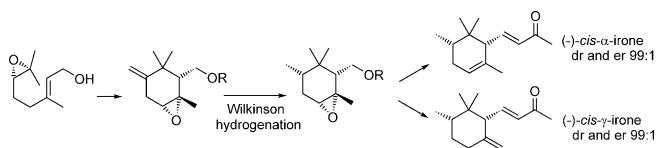
FULL PAPER

Total Synthesis

S. Bugoni, D. Boccato, A. Porta,*
G. Zanoni, G. Vidari*



Enantioselective Divergent Synthesis of (–)-*cis*-α- and (–)-*cis*-γ-Irone by Using Wilkinson's Catalyst



Science about scents: The well-known (–)-*cis*-α- and (–)-*cis*-γ-irone, the finest and strongest smell components of iris oils, have been synthesized in $\geq 99\%$ diastereomeric and enantioselective ratios. The diastereoselectivity of the

key Wilkinson's hydrogenation is supported by a detailed DFT modeling study of the geometry of the rhodium η^2 complexes involved in the diastereodifferentiation of the prostereogenic double bond faces.